Available online at www.sciencedirect.com
SCIENCE DIRECT®
International Journal of Mass Spectrometry 246 (2005) 49–55
International Journal of Mass Spectrometry
www.elsevier.com/locate/ijms

Electrospray ionization mass spectra of dinucleotide N3′ → P5′ phosphoramidates

Xu Tang [a,b], Hua Fu [a,*], Yu-Fen Zhao [a,b]

[a] *Key Laboratory of Bioorganic Phosphorus Chemistry of Education Ministry, Department of Chemistry, Tsinghua University, Beijing 100084, PR China*
[b] *Department of Chemistry, Xiamen University, Xiamen, Fujian 361005, PR China*

Received 7 June 2005; received in revised form 13 July 2005; accepted 13 July 2005
Available online 16 September 2005

Abstract

Dinucleotide N3′ → P5′ phosphoramidates were synthesized and determined by positive ion electrospray ionization mass spectrometry (ESI-MS), their fragmentation pathways were investigated using tandem mass spectrometric (MS/MS) techniques, and many abundant characteristic fragment ions were found. The results show that multistage ESI-MS is a powerful tool for the structure determination of dinucleotide N3′ → P5′ phosphoramidates.

Keywords: Dinucleotide N3′ → P5′ phosphoramidate; ESI-MS; Tandem mass spectrometry; Fragmentation pathway

1. Introduction

Nucleosides and nucleotides have demonstrated widespread utility as antiviral and anticancer therapeutics [1]. One of them is 3′-azido-2′,3′-dideoxythymidine (AZT) [2–4], which was the first clinically approved drug against HIV infection. The mechanism of action requires conversion of AZT to the corresponding 5′-mono-, di- and triphosphates by cellular kinases after cellular uptake [5]. AZT triphosphate then competes with dTTP for incorporation in viral DNA, leading to inhibition of reverse transcriptase and DNA chain termination. However, the long-term administration of nucleoside-based drugs can result in decreasing activity of kinases, thus, reducing their efficacy. For example, resistance to the antiviral activity of 3′-azido-3′-deoxythymidine [6,7] has been shown to arise from the decreased activity of the prerequisite first phosphorylating enzyme [8] and other side effects like bone marrow suppression, myopathy, hepatic abnormalities and so on [9]. In order to circumvent these problems and deliver the monophosphate efficiently into the target cell, a lot of work has been reported aimed at developing 5′-*O*-ester prodrugs of AZT [10–14].

Oligonucleotide N3′ → P5′ phosphoramidates have been attracted considerable attention as a class of compounds of potential therapeutic value [15–20], since these oligonucleotide analogues are resistant towards various nucleases [16,21] and hybridize to complementary DNA or RNA targets with much higher affinity than their natural congeners do [16]. In addition, 3′-amino-2′,3′-dideoxy-nucleoside analogue exhibit antitumor [22] and antiviral activity, which can conjugate with AZT or other anti-HIV nucleotides to be potential prodrugs and candidates for antisense purposes [23,24].

Electrospray ionization mass spectrometry has been widely used during recent years and become a useful tool for structural determination. For example, ESI-MS/MS has been applied to the determination of the DNA [25] and oligonucleotide [26–28] sequence. In our research group, the fragmentation pathways of AZT/d4T boranophosphates and dinucleotide thiophosphoramidates using ESI-MS/MS have been described [29,30]. Here, we would like to report the synthesis of several dinucleotide N3′ → P5′ phosphorami-

* Corresponding author. Tel.: +86 10 6277 2259; fax: +86 10 6278 1695.
E-mail address: fuhua@mail.tsinghua.edu.cn (H. Fu).

1387-3806/$ – see front matter © 2005 Elsevier B.V. All rights reserved.
doi:10.1016/j.ijms.2005.07.004

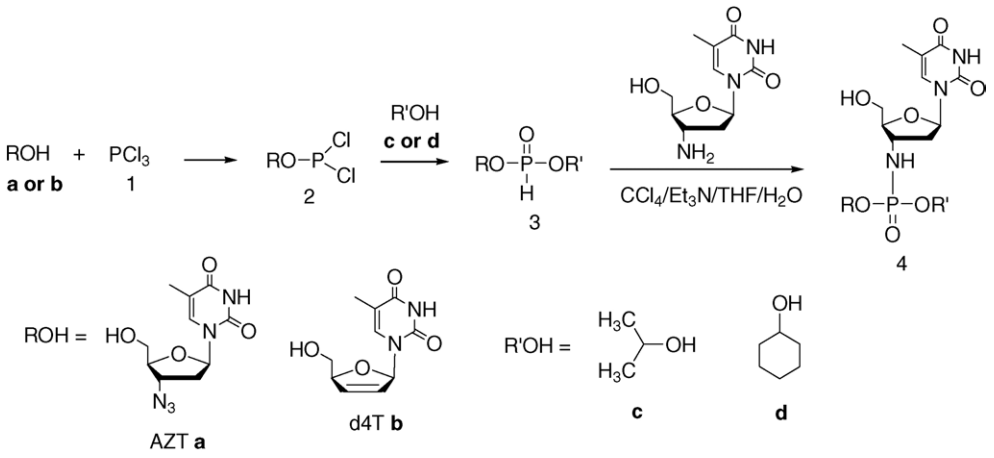

Scheme 1. Synthetic pathway of dinucleotide N3′ → P5′ phosphoramidates.

dates with potential anti-HIV activity and their fragmentation pathways in positive ion electrospray ionization (ESI) mass spectrometry combining with tandem mass spectrometry [31] (MS/MS) and quadrupole ion trap [32].

2. Experimental

2.1. Preparation of samples

5′-Hydrogenphosphonates **3** were synthesized as shown in Scheme 1 according to methods proposed in the literature [33,34]. The dinucleotide N3′ → P5′ phosphoramidates were obtained through Todd reaction, and general procedures are shown as follows.

2.2. Compound *3*

To a flask containing 1.38 g (10 mmol) PCl_3 in 10 mL dichloromethane, AZT (**a**) or d4T (**b**) was added in portions within 10 min at −30 °C. The reaction mixture was stirred at this temperature for 1 h and room temperature for 6 h. After the solvent and excess of PCl_3 were removed under reduced pressure, the residue was dissolved in 10 mL dichloromethane. Subsequently, 2.5 mmol alcohol in 3 mL dichloromethane was added dropwise to the solution on ice bath and stirred at 0 °C for 30 min, and then 2 mmol of Et_3N was dropped to the resulting solution. Ten minutes later, the solvent was removed in vacuo, and purification of the residue provided **3** by silica gel column chromatography using CH_2Cl_2/CH_3OH (20:1) as eluent.

2.3. Compound *4*

Compound **3** (0.36 mmol) in THF was added dropwise to 3′-aminothymindine (0.43 mmol) in mixed solvents of $THF/CCl_4/Et_3N/H_2O$ and stirred at room temperature for 1 h. After evaporation under reduced pressure, the residue was purified by silica gel column chromatography using CH_2Cl_2/CH_3OH (10:1) as solvents to give the target product **4** as colorless oil or white solid. Structure and purity of these compounds were checked by ^{31}P, ^{1}H and ^{13}C NMR.

2.4. Mass spectrometric conditions

The samples dissolved in methanol were continuously infused into the ESI chamber at a flow rate of 4 μL/min by a Cole-Parmer 74900 syringe pump (Cole-Parmer Instrument Company) and ionized by ESI. ESI mass spectra were acquired in positive ion mode using a Bruker ESQUIRE-LC^{TM} ion trap spectrometer equipped with a gas nebulizer probe. The capillary was typically held at 4 kV and the source temperature was maintained at 300 °C. The MS^n spectra were obtained by collision-induced dissociation (CID) with helium after isolation of the appropriate precursor ions.

3. Results and discussion

Here, ESI positive ion mass spectral fragmentation pathways of compound **4ad** is discussed as typical example. Other compounds have similar mass spectral fragmentation patterns.

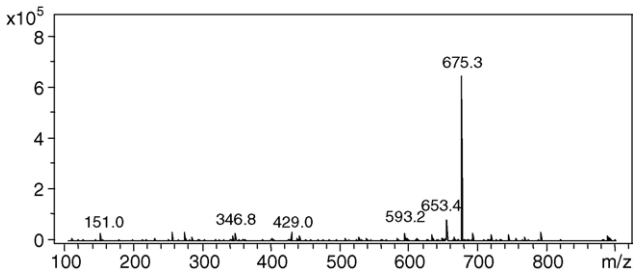

Fig. 1. Positive ion ESI mass spectrum of compound **4ad**.

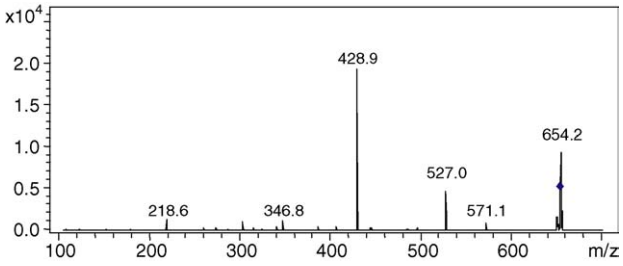

Fig. 2. ESI MS/MS mass spectrum of the protonated molecule at *m/z* 653 in Fig. 1 (corresponding to Scheme 2).

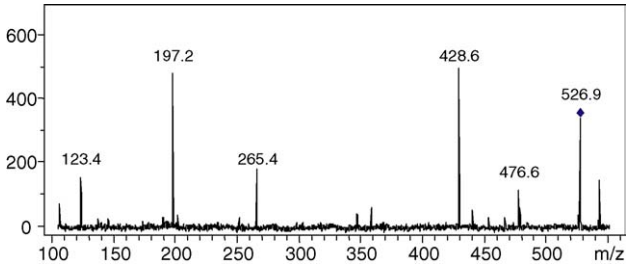

Fig. 3. The ESI-MS/MS/MS spectrum of the ion at *m/z* 527.

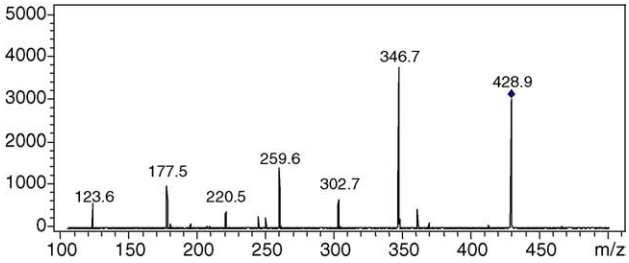

Fig. 4. The ESI-MS/MS/MS spectrum of the ion *m/z* 429.

*3.1. Positive ion mass spectrum of compound **4ad***

The mass spectrum of compound **4ad** (Fig. 1) shows the two main peaks at *m/z* 653 and 675 corresponding to the protonated and sodiated molecules $[M+H]^+$ and $[M+Na]^+$, respectively.

The ESI-MS/MS fragmentation of the protonated molecule at *m/z* 653 (Fig. 2) is summarized in Scheme 2. The ions at *m/z* 571 corresponding to cyclohexene loss from $[M+H]^+$, *m/z* 527 and 429 corresponding to $[MH-\text{thymine}]^+$ and $[MH-\text{d4T}]^+$ (d4T 2′,3′-didehydro-3′-deoxythymidine) were observed, respectively.

The ESI-MS/MS/MS spectrum of the ion *m/z* 527 (Fig. 3), summarized in Scheme 3, produced ion at *m/z* 429 which was also observed in the ESI-MS/MS spectrum of $[M+H]^+$ at *m/z* 653 (Scheme 2). Two odd-electron ions at *m/z* 197 and 123 were observed, which came from loss of radical fragments, and the similar results were found in other paper [35].

The ESI-MS/MS/MS spectrum of the ion at *m/z* 429 is shown in Fig. 4 followed by the pathway of the ion (Scheme 4). $[M-\text{d4T}-\text{cyclohexene}]^+$ was observed at *m/z* 347. The ion at *m/z* 303 came from loss of thymine, and the ion at *m/z* 260 corresponded to neutral molecule HN_3 and thymine loss from the precursor ion. The ion at *m/z* 178 came from the parent ion by losing thymine, HN_3 and cyclohexene. The ion at *m/z* 124 was $[\text{AZT}-H_2O-\text{thymine}+H]^+$.

The ESI-MS/MS/MS/MS spectrum of the ion at *m/z* 347 is shown in Fig. 5, and the fragmentation pathway of the ion at *m/z* 347 is displayed in Scheme 5. A peak at *m/z* 221 was observed corresponding to thymine loss from the parent ion. Meanwhile, we also observed peaks at *m/z* 204 and 178, which corresponded to $[\text{precursor ion}-\text{thymine}-NH_3]^+$ and $[\text{precursor ion}-\text{thymine}-HN_3]^+$, respectively. In addition, a

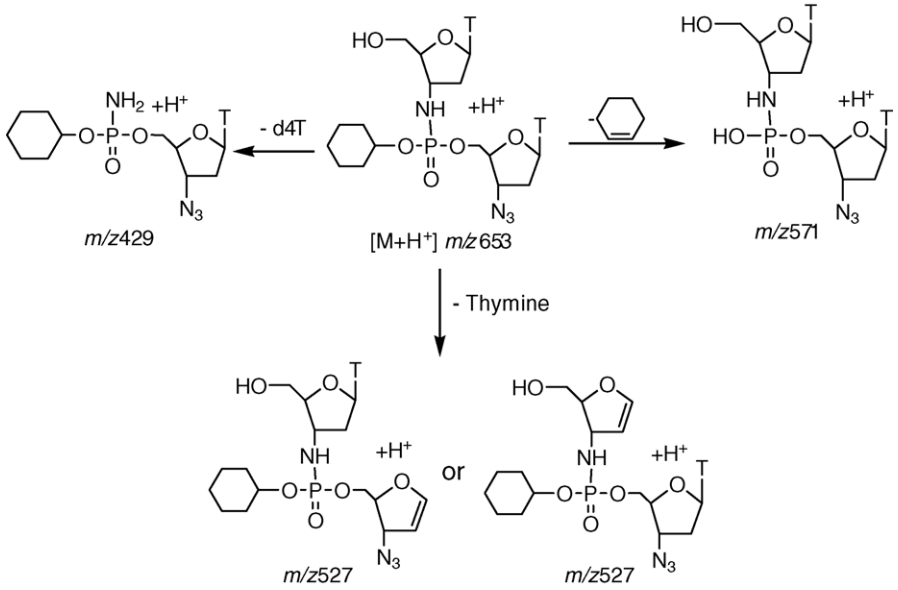

Scheme 2. ESI-MS/MS fragmentation pathway of the ion at *m/z* 653.

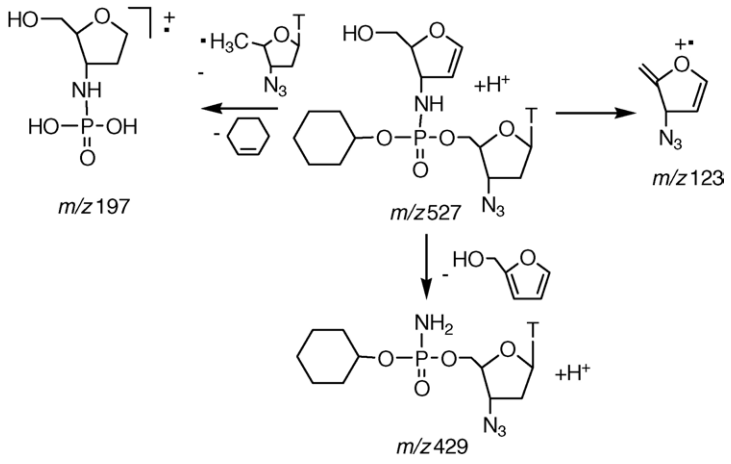

Scheme 3. ESI-MS/MS/MS fragmentation pathway of the ion at *m/z* 527.

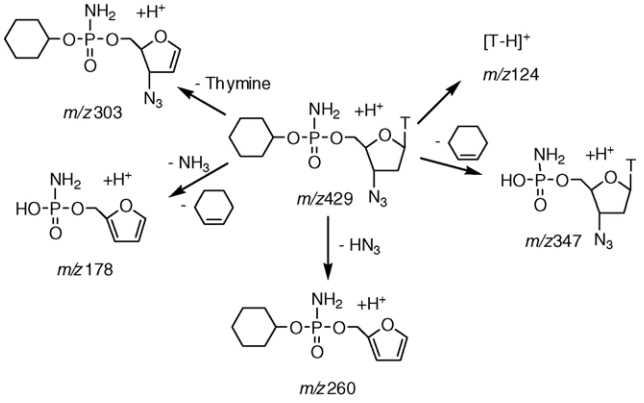

Scheme 4. ESI-MS/MS/MS fragmentation pathway of the ion at *m/z* 429.

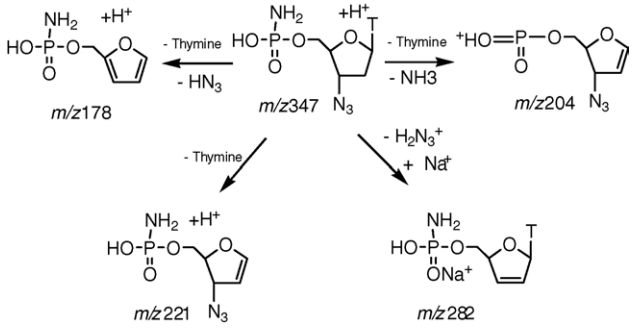

Scheme 5. The fragmentation pathway of the ion at *m/z* 347.

novel rearrangement ion at *m/z* 282 was observed, and its possible formation mechanism is proposed in Scheme 6. The cleavage of C–O bond on furan and the new five-membered ring in ion **A** at *m/z* 347 produced the intermediate **B**, the subsequent proton migration and cleavage of bonds yielded ion E at *m/z* 282 by losing $PONH_4$ from ion A at *m/z* 347.

In this paper, the ESI-MS^n spectra of the sodiated molecule $[M + Na]^+$ at *m/z* 575 were also undertaken.

The ESI-MS/MS spectrum of $[M + Na]^+$ and the fragmentation pathway are shown in Fig. 6 and Scheme 7. When the ion $[M + Na]^+$ lost cyclohexene, the ion at *m/z* 593 can be observed. Fragment ion at *m/z* 426 was observed corresponding to the cleavage of 5′C–O bond. If the two steps were taken simultaneously, the ion at *m/z* 344 can be generated. The ions at *m/z* 264 and 229 corresponding to [3′-amino-2′,3′-dideoxythymidine + Na]$^+$ and $[d4T - H_2O + Na]^+$ were observed. The ion at *m/z* 324 came from the cyclohexene and hydroxyl radical losses from precursor ion.

The ESI-MS/MS/MS spectrum of the ion at *m/z* 344 (Fig. 7), summarized in Scheme 8, produced ion at *m/z* 229 and 264 which were also observed in the ESI-MS/MS spectrum of the ion at *m/z* 675 (Scheme 7). The new ion at *m/z* 218 was attributed to thymine loss from the precursor ion.

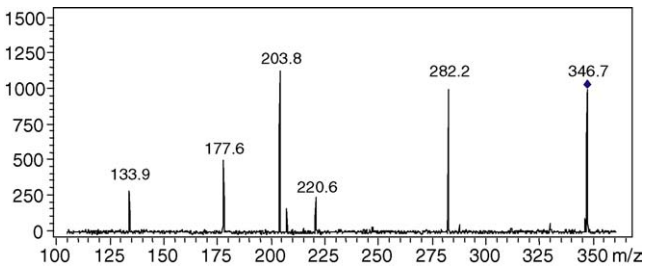

Fig. 5. The ESI-MS/MS/MS/MS spectrum of the ion at *m/z* 347.

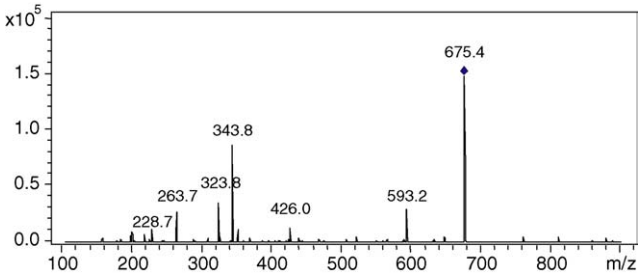

Fig. 6. ESI-MS/MS spectrum of ion at *m/z* 675.

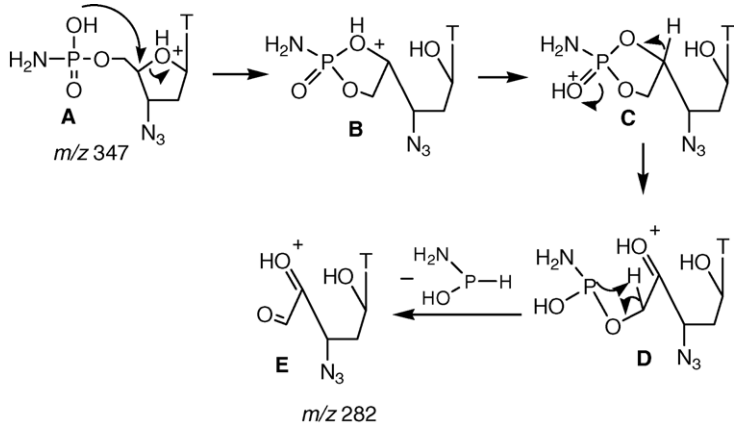

Scheme 6. Possible formation mechanism of the ion at *m*/*z* 282 from the ion at *m*/*z* 347.

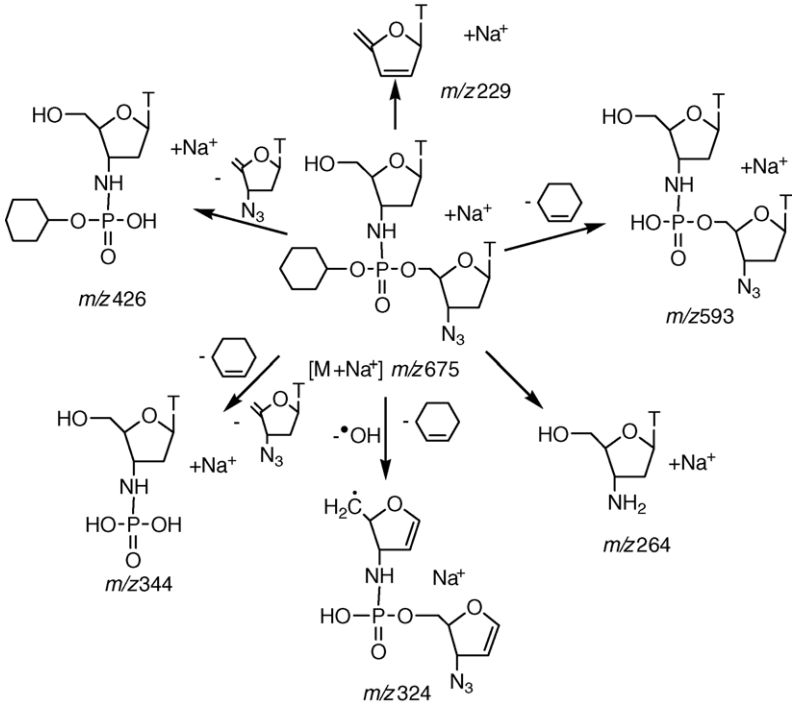

Scheme 7. The fragmentation pathway of the ion at *m*/*z* 675.

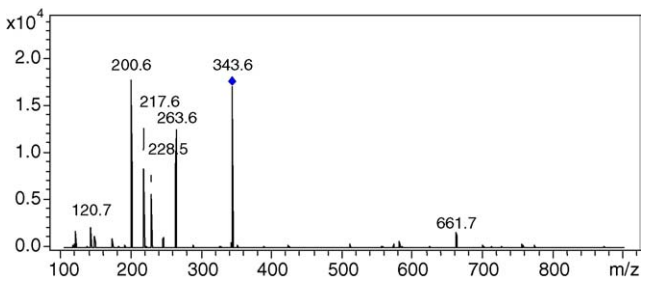

Fig. 7. ESI-MS/MS/MS spectrum of ion at *m*/*z* 344.

The ion at *m*/*z* 121 was attributed to thymine loss and the cleavage of 3′C–3′N bond. In addition, the radical ion at *m*/*z* 201 was observed.

ESI-MS/MS/MS spectrum of the sodiated 3′-aminothymindine at *m*/*z* 264 is shown in Fig. 8 and summarized in Scheme 9. The ion at *m*/*z* 138 was generated from the thymine loss, and its complementary ion at *m*/*z* 149 was observed. The ion at *m*/*z* 123 was attributed to thymine loss and cleavage of 3′C–3′N bond.

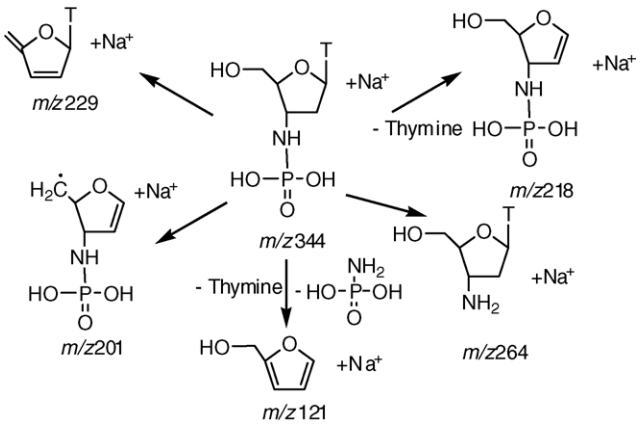

Scheme 8. The ESI-MS/MS/MS spectral fragmentation pathway of the ion at *m*/*z* 344.

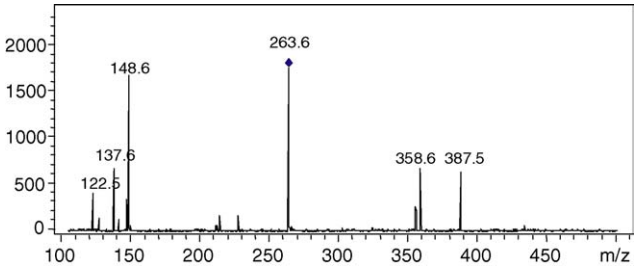

Fig. 8. ESI-MS/MS/MS/MS spectrum of ion at *m*/*z* 264.

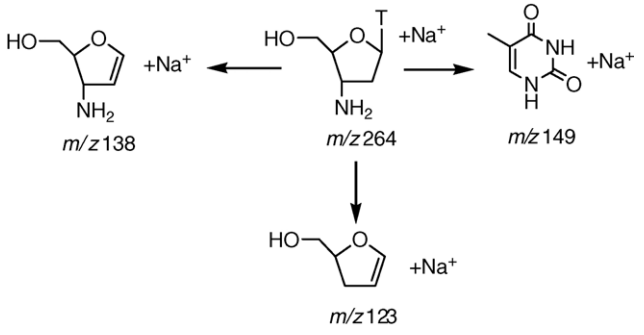

Scheme 9. The ESI-MS/MS/MS/MS spectral fragmentation pathway of the ion at *m*/*z* 264.

4. Conclusions

Positive ion electrospray ionization mass spectra of dinucleotide N3′ → P5′ phosphoramidates produced ions corresponding to losses of d4T, thymine, cyclohexene and cleavage of P–N bond and O–5′C bond. Multistage mass spectrometry of electrospray ionization can provide abundant characteristic fragment ion information, which is very helpful tool for structural elucidation of these compounds.

Acknowledgements

This work was supported by the Excellent Dissertation Foundation of the Chinese Ministry of Education (No. 200222), the Excellent Young Teacher Program of MOE, P. R. C., and the National Natural Science Foundation of China (Grant No. 20472042).

Appendix A. Appendix A

Spectra, for example, compound **4ad**.

^{31}P NMR (DMSO-d_6, 121.5 MHz) δ 9.05 ppm (s); ^{1}H NMR (DMSO-d_6, 300 MHz) δ 1.24–1.29, 1.43–1.46, 1.55–1.7, 1.77–1.9 (m, 11H, C_6H_{11}–), 1.77 (s, 3H, CH_3–), 1.80 (s, 3H, CH_3–), 2.1–2.2 (m, 2H, 2′-CH_2), 2.25–2.45 (m, 2H, 2′-CH_2), 3.1–3.2 (m, 1H, 3′-NH), 3.48–3.58 (m, 1H, –CH_2–C<u>H</u>–CH_2–), 3.6–3.85, 3.9–4.1, 4.1–4.3, 4.32–4.52 (m, 8H, 3′, 4′, 5′-H), 4.95–5.1 (m, 1H, 5′-OH), 6.13 (t, 2H, 1′-H, J_{H-H} = 6.25 Hz), 7.53 (s, 1H, 5-H of AZT), 7.73 (s, 1H, 5-H of 3′-amino-2′,3′-dideoxythymidine), 11.27 (s, 1H, 3-NH of AZT), 11.36 (s, 1H, 3-NH of 3′-amino-2′,3′-dideoxythymidine). ^{13}C NMR (DMSO-d_6, 75 MHz) δ 12.16, 12.28, 23.06, 24.79, 32.96, 33.00, 35.75, 50.64, 60.32, 60.59, 65.01, 75.07, 81.64, 81.74, 83.41, 83.77, 85.86, 109.26, 110.02, 135.93, 136.26, 150.42, 163.71, 163.80.

References

[1] R.J. Jones, N. Bischofberger, Antiviral Res. 27 (1995) 1.
[2] B.D. Cheson, M.J. Keating, W. Plunkett, Nucleoside Analogs in Cancer Therapy, Marcel Dekker, New York, 1990.
[3] E. De Clercq, Nucleosides Nucleotides 13 (1994) 1271.
[4] P. Herdewijn, Drug Discov.Today 2 (1997) 235.
[5] J. Kim, S. Park, N.Y. Tretyakova, C.R. Wagner, Mol. Pharmcol. 2 (2004) 233.
[6] G. Antonelli, O. Turriziani, A. Verri, P. Narciso, F. Ferri, G. D'Offizi, F. Dianzini, AIDS Res. Hum. Retroviruses 12 (1996) 223.
[7] G. Hoever, B. Groeschel, P. Chandra, H.W. Doerr, Int. J. Mol. Med. 11 (2003) 743.
[8] J. Kim, T. Chou, G.W. Griesgraber, C.R. Wagner, Mol. Pharmcol. 1 (2004) 102.
[9] K.H.P. Moore, Rh. Raasch, K.L.R. Brouwer, K. Opheim, S.H. Cheeseman, E. Eyster, S.M. Lemon, C.M. Vanderhorst, Antimicrob. Agents Chemother. 39 (1995) 2732.
[10] C. Meier, Synlett 1998 (1998) 233.
[11] C.R. Wagner, V.V. Iyer, E.J. McIntee, Med. Res. Rev. 20 (2000) 417.
[12] D.P. Drontle, C.R. Wagner, Mini-Rev. Med. Chem. 4 (2004) 409.
[13] K. Parang, L.I. Wiebe, E.E. Knaus, Curr. Med. Chem. 7 (2000) 995.
[14] C.R. Wagner, V.V. Iyer, E.J. McIntee, Med. Res. Rev. 20 (2000) 417.
[15] S.M. Gryaznov, T. Skórski, C. Cucco, M. Nieborowska-Skórska, C.Y. Chin, D. Lloyd, J.-K. Chen, M. Koziólkiewicz, B. Calabretta, Nucleic Acids Res. 24 (1996) 1508.
[16] M.L. Riordan, J.C. Martin, Nature 350 (1991) 442.
[17] S.M. Gryaznov, D.H. Lloyd, J.-K. Chen, R.G. Schultz, L.A. DeDionisio, L. Ratmeyer, W.D. Wilson, Proc. Natl. Acad. Sci. U.S.A. 92 (1995) 5798.
[18] C. Giovannangeli, S. Diviacco, V. Labrousse, S. Gryaznov, P. Charneau, C. Helene, Proc. Natl. Acad. Sci. U.S.A. 94 (1997) 79.
[19] S.M. Gryaznov, R.L. Letsinger, Nucleic Acids Res. 20 (1992) 3403.

[20] C.T. Rigl, D.H. Lloyd, D.S. Tsou, S.M. Gryaznov, W.D. Wilson, Biochemistry 36 (1997) 650.
[21] C. Escude, C. Giovannangeli, J.S. Sun, D.H. Lloyd, J.K. Chen, S.M. Gryaznov, T. Garestier, C. Helene, Proc. Natl. Acad. Sci. U.S.A. 93 (1996) 4365.
[22] T.S. Lin, W.R. Mancini, J. Med. Chem. 26 (1983) 544.
[23] S.M. Gryaznov, H. Winter, Nucleic Acids Res. 26 (1998) 4160.
[24] T.J. Matray, S.M. Gryaznov, Nucleic Acids Res. 27 (1999) 3976.
[25] K.K. Murray, J. Mass Spectrom. 31 (1996) 1203.
[26] J.S. Ni, S.C. Pomerantz, J. Rozenski, Y.H. Zhang, J.A. McCloskey, Anal. Chem. 68 (1996) 1989.
[27] J.S. Ni, M.A.A. Mathews, J.A. McCloskey, Rapid Commun. Mass Spectrom. 11 (1997) 535.
[28] S.C. Pomerantz, J.A. McCloskey, T.M. Tarasow, B.E. Eaton, J. Am. Chem. Soc. 119 (1997) 3861.
[29] C.X. Lin, H. Fu, Y.F. Zhao, Rapid Commun. Mass Spectrom. 18 (2004) 273.
[30] C.X. Lin, H. Fu, Y.F. Zhao, Rapid Commun. Mass Spectrom. 19 (2005) 292.
[31] E. de Hoffmann, J. Mass Spectrom. 31 (1996) 129.
[32] R.E. March, J. Mass Spectrom. 32 (1997) 351.
[33] X.B. Sun, J.X. Kang, Y.F. Zhao, Chem. Commun. 20 (2002) 2414.
[34] G.J. Ji, C.B. Xue, J.N. Zeng, L.P. Li, W.G. Chai, Y.F. Zhao, Synthesis 1988 (1988) 444.
[35] M.J. Chalmers, K. Hakansson, R. Johnson, R. Smith, J.W. Shen, M.R. Emmett, A.G. Marshall, Proteomics 4 (2004) 970.